Astron. Astrophys. 326, 277–286 (1997)

ASTRONOMY
AND
ASTROPHYSICS

Spherically symmetric model atmospheres using approximate lambda operators

III. The equations of statistical equilibrium with occupation probabilities

Jiří Kubát

Astronomický ústav, Akademie věd České republiky, 251 65 Ondřejov, Czech Republic

Received 7 March 1997 / Accepted 22 April 1997

Abstract. The occupation probability formalism is implemented into the equations of statistical equilibrium. The equations and corresponding expressions for rates are presented in detail. The improved equations are used for the calculation of sample spherically symmetric NLTE model atmospheres. The difference between this formalism and standard cutoff formula is studied for pure hydrogen atmospheres. It is small for main-sequence and sdO stars. However, a larger difference is found for white dwarfs.

Key words: stars: atmospheres – atomic processes – methods: numerical

1. Introduction

In our previous papers (Kubát 1994 – hereinafter Paper I, Kubát 1996 – hereinafter Paper II) we have presented a description of a method for the calculation of static spherically symmetric NLTE model atmospheres in radiative and hydrostatic equilibrium. The equations of hydrostatic equilibrium, radiative equilibrium, and radiative transfer were described in detail in Papers I and II. Here we shall discuss only the equations of statistical equilibrium and underlying expressions for opacities and emissivities using the occupation probability formalism of Hummer & Mihalas (1988).

Calculations of model stellar atmospheres using classical expressions for opacities (see Mihalas 1978, Eq.7.1) and standard cutoff formula for partition functions (see Traving et al. 1966) yield reliable model atmospheres that give satisfactory agreement with observations (for a review see Kudritzki & Hummer 1990). The standard cutoff formula for calculation of a partition function implicitly assumes that for given temperature and density all the atoms in a particular ionization stage have exactly the same number of non-dissolved atomic levels. Nevertheless, this procedure for calculation of a partition function introduces systematic errors into ionization balance, and consequently the electron density. Therefore it is natural to try to replace the above mentioned standard cutoff procedure by a more accurate one. An extended discussion of various cutoff methods was published by Däppen et al. (1987). Hummer & Mihalas (1988) proposed to replace the assumption of the same number of non-dissolved levels for all atoms in a particular ionization stage by a smooth distribution of a number of non-dissolved levels. They used this occupation probability formalism as a cutoff procedure in the partition function calculations. Using this formalism, Mihalas et al. (1988, 1990) and Däppen et al. (1988) calculated illustrative examples of ionization fractions as well as thermodynamic quantities for several values of temperature and density, and different chemical composition. Hubeny et al. (1994 – hereinafter HHL) applied this approach to stellar opacities near series limit and demonstrated the usefulness of the occupation probabilities for calculations. Recently, the implementation of this formalism into the NLTE plane-parallel code was briefly described by Werner (1996). In this paper we use the method of HHL for calculations of static spherically symmetric model atmospheres.

2. The equations of statistical equilibrium

2.1. LTE ionization and excitation equilibrium

As in HHL we use the partition function in the form

$$Z = \sum_{i=1}^{\infty} w_i g_i e^{-E_i/kT},$$

where E_i is the excitation energy of level i, g_i is the statistical weight, w_i is the occupation probability, and T is the temperature. The LTE population number n_i^* is then

$$n_i^* = \frac{N^*}{Z} w_i g_i e^{-E_i/kT}. \quad (1)$$

Here N^* is the total LTE number density of the corresponding ion that can be calculated from the Saha equation

$$\frac{N_j^*}{N_{j+1}^*} = n_e \frac{Z_j}{Z_{j+1}} C_S T^{-3/2} e^{-E_j/kT}, \tag{2}$$

where n_e is the electron density, E_j is the ionization energy, and $C_S = 0.5(h^2/(2\pi m_e k))^{3/2}$. Eq.(2) underlines the necessity of a proper treatment of a partition function, since it directly affects the ionization equilibrium, and consequently level population numbers. Commonly used polynomial fits to the partition function of Traving et al. (1966) introduce systematic errors (depending on the values of temperature and electron density) into calculations, which may be several orders of magnitude (in the worst cases). Luckily, their effect on the resulting model need not be so drastic, since the changes in the dominant element (hydrogen) in the standard atmosphere affect only H I, while prevailing ionization stage is H II. Therefore, the total amount of free electrons practically does not change. In any case, using of the occupation probabilities is superior to the standard cut-off procedure, especially in such situations when two ionization stages of the same element compete.

2.2. NLTE ionization and excitation equilibrium (statistical equilibrium)

We express the NLTE population numbers with the help of departure coefficients (b-factors), defined as $b_i = n_i/n_i^*$ by Menzel (1937). The NLTE ionization and excitation equilibrium is described by a set of equations of statistical equilibrium (see, e.g. Mihalas 1978)

$$\mathscr{A}_{il} \cdot b_l = \mathscr{B}_i. \tag{3}$$

In the following subsections we will describe this set of equations in detail.

2.2.1. Rate equations

The rate equations for the static case using occupation probabilities w_i can be written as (see HHL)

$$b_i n_i^* \sum_l w_l (R_{il} + C_{il}) - w_i \sum_l b_l n_l^* (R_{li} + C_{li}) = 0. \tag{4}$$

We rewrite the Eq.(4) in the form

$$b_i \sum_l (\tilde{R}_{il} + \tilde{C}_{il}) - \sum_l b_l (\tilde{R}_{li} + \tilde{C}_{li}) = 0, \tag{5}$$

where we have introduced the quantities $\tilde{R}_{il} = n_i^* w_l R_{il}$ and $\tilde{C}_{il} = n_i^* w_l C_{il}$. We will refer to these quantities as to the *weighted rates*. Particular expressions for these rates are

$$\tilde{R}_{il} = n_i^* w_l \frac{4\pi}{h\nu_{il}} \int_0^\infty \sigma_{il}(\nu) J_\nu \mathrm{d}\nu \tag{6}$$

for upward bound-bound radiative rates,

$$\tilde{R}_{li} = n_l^* w_i \frac{g_i}{g_l} \frac{4\pi}{h\nu_{il}} \int_0^\infty \sigma_{il}(\nu) \left(\frac{2h\nu^3}{c^2} + J_\nu \right) \mathrm{d}\nu \tag{7}$$

for downward bound-bound radiative rates

$$\tilde{R}_{ik} = 4\pi n_i^* w_k \int_0^\infty \frac{\sigma_{ik}(\nu)}{h\nu} J_\nu \mathrm{d}\nu \tag{8}$$

for upward bound-free radiative rates, and

$$\tilde{R}_{ki} = 4\pi n_i^* w_i \int_0^\infty \frac{\sigma_{ik}(\nu)}{h\nu} \left(\frac{2h\nu^3}{c^2} + J_\nu \right) e^{-h\nu/kT} \mathrm{d}\nu \tag{9}$$

for free-bound radiative rates. Here σ_{il} stands for the general cross-section (both bound-free and free-free) for transitions between levels i and l.

The upward and downward weighted collisional rates (both excitation and ionization) are written as (see Mihalas 1978)

$$\tilde{C}_{il} = \tilde{C}_{li} = n_e n_i^* w_l q_{il}(T). \tag{10}$$

Here $q_{il}(T)$ is the collision excitation rate coefficient (Gallagher & Pradhan 1985). Let us finally express the particular coefficients of the rate matrix $\mathscr{A}$ explicitly. The off-diagonal elements of the rate matrix read

$$\mathscr{A}_{il(i\neq l)} = -(\tilde{R}_{li} + \tilde{C}_{li}) \tag{11}$$

and the diagonal elements are

$$\mathscr{A}_{ii} = \sum_{l=1}^{NL} (\tilde{R}_{il} + \tilde{C}_{il}), \tag{12}$$

where the quantities $\tilde{R}$ and $\tilde{C}$ are introduced in the Eq.(5). The right hand side of the rate equations $\mathscr{B}$ is zero.

2.2.2. Closing equations

Since the system of rate equations is linearly dependent (see e.g. Mihalas 1978), we close it with the help of either the particle conservation equation

$$\sum_k N_k = N - n_e \tag{13}$$

or the charge conservation equation

$$\sum_k \sum_j q_j N_{jk} = n_e. \tag{14}$$

Here N_k is the number density of an atom k, N_{jk} is the number density of an ion j (of an atom k), q_j is the ionization degree of an ion j, and N is the total number density. If we consider more than one element (usually hydrogen), we have to close the equations of statistical equilibrium for each element. We use the abundance equation

$$N_k = Y_k N_r, \tag{15}$$

where N_r is the number density of a reference element (usually hydrogen), and Y_k is the abundance relative to this element.

For each element we must replace one of the rate equations with one of Eqs.(13), (14), or (15). The common choice (also adopted by us) is to replace the last equation for the reference element (e.g. hydrogen, but use of other elements is also possible) optionally either with Eq.(13) or with Eq.(14) and for all other elements except the reference one with Eq.(15).

The densities and population numbers vary by several orders of magnitude throughout the atmosphere, and consequently the right hand side of the equations (13) – (15) varies in the same way. Since we solve the equations for the *b*-factors and not for the population numbers, it is numerically convenient to divide these equations by the massive particle density

$$n_m = \frac{\sum_k Y_k m_k N_k}{\sum_k Y_k m_k},$$

where summation goes over all elements included and m_k is the mass of a particular element. Then the right hand side is of the order of 1 in the whole atmosphere. Let us list matrix coefficients for these equations. For Eq.(13) we have (asterisks mean LTE populations)

$$\mathscr{A}_{rl} = \frac{n_l^*}{n_m} \tag{16}$$

with the right hand side

$$\mathscr{B}_r = 1. \tag{17}$$

Similarly, Eq.(14) yields

$$\mathscr{A}_{rl} = q_l \frac{n_l^*}{n_m} \tag{18}$$

with the right hand side

$$\mathscr{B}_r = \frac{n_e}{n_m}. \tag{19}$$

Finally, for the abundance equation (15) we have

$$\begin{aligned} \mathscr{A}_{rl} &= \frac{n_l^*}{n_m} \quad \text{for the element being closed} \\ &= -\frac{n_l^*}{n_m} \quad \text{for the reference element} \\ &= 0 \qquad \text{for the rest} \end{aligned} \tag{20}$$

with the right hand side

$$\mathscr{B}_r = 0. \tag{21}$$

2.3. Opacities with occupation probabilities

We include the occupation probability formalism in the expressions for opacities basically after HHL. The bound-bound opacity with occupation probabilities for a transition from level i to level j is

$$\chi_{il}(\nu) = \left(n_i^* b_i w_l - n_l^* b_l w_i\right) \sigma_{il}(\nu). \tag{22}$$

The bound-bound cross-section $\sigma_{il}(\nu)$ is

$$\sigma_{il}(\nu) = \frac{\pi e^2}{m_e c} f_{il} \phi_{il}(\nu), \tag{23}$$

where f_{il} is the oscillator strength, and $\phi_{il}(\nu)$ is a line profile. The opacity for photoionization (bound-free) transitions is then

$$\chi_{ik}(\nu) = n_i^* \left(b_i w_k - b_k w_i e^{-h\nu/kT}\right) \tilde{\sigma}_{ik}(\nu) \tag{24}$$

where the extrapolated cross-section (for a discussion of this see Däppen et al. 1987 and HHL)

$$\begin{aligned} \tilde{\sigma}_{ik}(\nu) &= \sigma_{ik}(\nu) \qquad\qquad \text{for} \quad \nu \geq \nu_{ik} \\ &= \left(1 - \frac{w_{n^*}}{w_i}\right) \sigma_{ik}(\nu) \quad \text{for} \quad \nu < \nu_{ik}. \end{aligned} \tag{25}$$

The effective quantum number n^* is generally a non-integer quantum number of the fictitious highest state that can be reached from the state i by the absorption of a photon of a energy of $h\nu$ (Däppen et al 1987)

$$n^* = \left(\frac{1}{n_i^2} - \frac{h\nu}{\chi_{\rm ION}}\right).$$

where n_i is the quantum number of the level i and $\chi_{\rm ION}$ in the ionization energy. The occupation probability w_{n^*} is calculated similarly as the occupation probabilities w_i using the formulae in the Appendix of HHL. For a calculation of the photoionization cross-section $\sigma_{ik}(\nu)$ for frequencies below the ionization edge we may simply use the standard formula in Mihalas (1978).

The expression for free-free transitions

$$\chi_{kk}(\nu) = n_e b_k n_k^* \sigma_{kk}(\nu, T) \left(1 - e^{-h\nu/kT}\right) \tag{26}$$

is not directly affected by the presence of the occupation probabilities in our method. The effect of the occupation probabilities is, however, indirect, since changes in photoionization cross-section (and consequently in bound-free rates) cause changes in the number of free electrons and population numbers.

3. Computational details

The method of solution has been described in detail in Papers I and II. Here we discuss only some particular details, which we regard to be important.

3.1. Radiative transfer

The radiative transfer equation in the linearization step is treated with the help of approximate lambda operators, i.e. the mean intensity of radiation is expressed as

$$J_\nu = \Lambda_\nu^* S_\nu + \left(\Lambda_\nu - \Lambda_\nu^*\right) S_\nu = \Lambda_\nu^* S_\nu + \Delta J_\nu. \tag{27}$$

The approximate diagonal or tridiagonal lambda operator Λ^* is calculated for both geometries using the short characteristics method of Olson & Kunasz (1987). We also implemented a

possibility to calculate a Λ^* operator after the formal solution of the transfer equation following the idea of Rybicki & Hummer (1991) and Puls (1991).

The formal solution of the transfer equation is calculated using either 2nd order differences (Mihalas 1985), splines, or Hermite solution (Auer 1976) using Feautrier (1964) variables. More details about the radiative transfer in our code can be found in Papers I and II.

3.2. Linearization of the equations of statistical equilibrium

The equations of statistical equilibrium closed with the particle (or charge) conservation equation and the abundance equations (if more elements than hydrogen enter the calculation) can be formally expressed as

$$\mathscr{A} \cdot \boldsymbol{b} = \mathscr{B}. \tag{28}$$

3.2.1. Explicit linearization of the *b*-factors

Since these equations are non-linear, they are to be linearized together with the equations of hydrostatic and radiative equilibrium, and with an equation for the radius. The linearized Eq.(28) is

$$\delta\mathscr{A} \cdot \boldsymbol{b} + \mathscr{A} \cdot \delta\boldsymbol{b} - \delta\mathscr{B} = \mathscr{B} - \mathscr{A} \cdot \boldsymbol{b}. \tag{29}$$

The detailed form of this equation is given in the Appendix. The quantities we want to determine in the linearization step are n_e, T, r (for spherical atmospheres only), and b_i. The standard way is to linearize the equations of radiative, hydrostatic, and statistical equilibrium and to solve the resulting linearized equations for corrections δn_e, δT, and δb_i. In total we must construct and solve $NL+2$ linearized equations. Then, in order to stabilize the solution, it is recommended (Auer & Mihalas 1969b, Mihalas & Auer 1970 – and we do the same) not to use the new values $b_i^{\rm new} = b_i^{\rm old} + \delta b_i$, but to calculate them using the equations of statistical equilibrium with the new values of n_e and T. We shall call this method the explicit linearization of the *b*-factors.

3.2.2. Implicit linearization of the *b*-factors

As an alternative it is possible to express

$$\delta b_i = \frac{\partial b_i}{\partial n_e}\delta n_e + \frac{\partial b_i}{\partial T}\delta T + \frac{\partial b_i}{\partial r}\delta r \tag{30}$$

and use this expression in linearized equations of hydrostatic and radiative equilibrium in order to eliminate δb_i. The derivatives of the *b*-factors vs. electron density, temperature, and radius are expressed from the equations of statistical equilibrium using the equation (ψ stands for r, n_e, and T)

$$\frac{\partial \boldsymbol{b}}{\partial \psi} = - \left(\mathscr{A} + \frac{\partial \mathscr{A}}{\partial \boldsymbol{b}} \cdot \boldsymbol{b} - \frac{\partial \mathscr{B}}{\partial \boldsymbol{b}} \right)^{-1} \cdot \left(\frac{\partial \mathscr{A}}{\partial \psi} \cdot \boldsymbol{b} - \frac{\partial \mathscr{B}}{\partial \psi} \right). \tag{31}$$

(see Eq.30 in Paper I). Then the linearized *b*-factors are eliminated using the relation (30). Then, as in the explicit linearization, the new *b*-factors are calculated using the equations of statistical equilibrium. This method will be called here the implicit linearization of *b*-factors. In practice, it is sufficient (and sometimes more stable) to neglect the dependence of $\mathscr{A}$ and $\mathscr{B}$ on *b*-factors and to use the simpler relation

$$\frac{\partial \boldsymbol{b}}{\partial \psi} = - \left(\frac{\partial \mathscr{A}}{\partial \psi} \cdot \boldsymbol{b} - \frac{\partial \mathscr{B}}{\partial \psi} \right). \tag{32}$$

The resulting system of linearized equations is very small, since the changes of the *b*-factors are not calculated explicitly and we can arrive at a very attractive number of only three variables (n_e, T, r). However, it is clear that this method of the linearization of the *b*-factors can not serve as a tool for the solution of a so-called restricted NLTE problem, i.e the solution of the coupled statistical equilibrium and radiation transfer equations when the atmospheric structure (T, n_e, r, ...) is given. On the other hand, the explicit linearization does not suffer from the latter drawback, but we have to linearize (and solve) more equations.

3.2.3. Comparison of both methods

At first sight one would expect the following conclusion (similar to that of Paper I): The implicit linearization is faster in CPU than the explicit one since we solve substantially smaller set of equations. On the other hand, the explicit linearization is faster numerically, since it takes the coupling between radiation field and atomic level populations directly into account. Nevertheless, a period of testing of both methods did not confirm preceding conclusions completely.

For calculations of model atmospheres of hot white dwarfs (Kubát 1995, 1997) we successfully used the explicit linearization. The implicit linearization served sometimes as an acceleration tool since it produced larger corrections when they were necessary and the explicit linearization was used for fine tuning of models. On the other hand, for some other stellar parameters the implicit linearization failed to converge. This is not too surprising since larger corrections may get out of hand. More interesting is the fact that sometimes we observed just opposite behaviour, i.e. explicit linearization failed while the implicit one successfully converged. This happened for some models of main sequence A stars.

The reason for such a strange behaviour is not too clear. Here we can conclude only with a need to test these two alternatives more systematically in future.

4. Results and discussion

In order to test the effect of a better treatment of the level dissolution by means of the occupation probability formalism we calculated a small set of representative models. For the sake of testing we included only hydrogen in our calculations. All models have 16 NLTE levels of H I and 1 level of H II. The line oscillator strengths were taken from Wiese et al. (1966), the lines

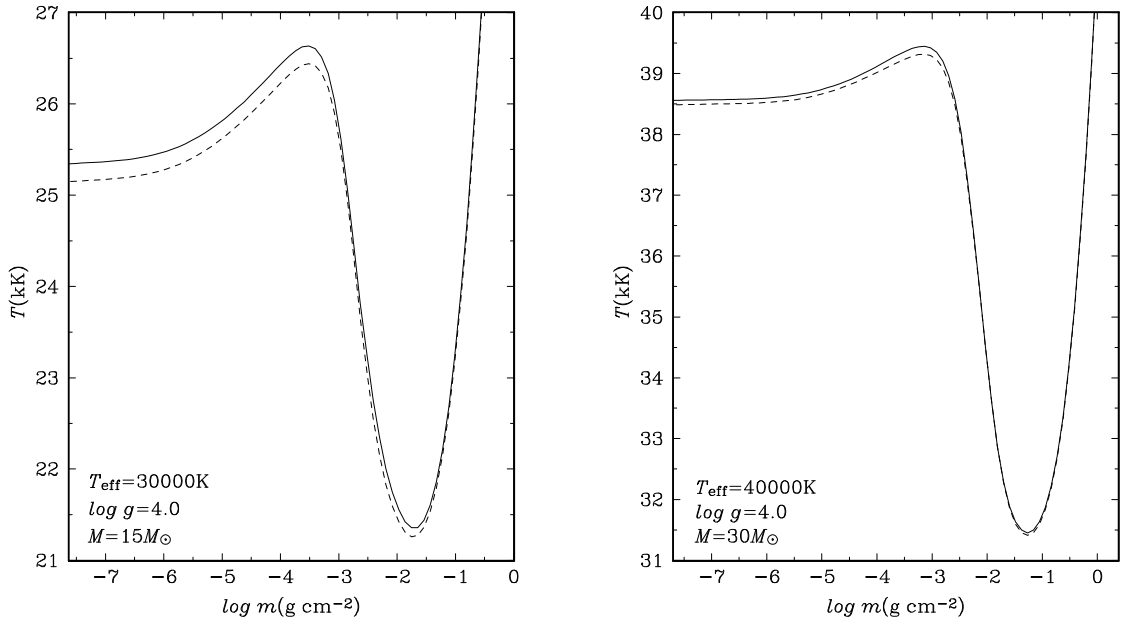

Fig. 1. Outer regions of spherically symmetric NLTE model atmospheres of a main-sequence B star ($T_{\rm eff}$ = 30000K, $\log g$ = 4.0, $M = 15M_{\odot}$), and of a main-sequence O star ($T_{\rm eff}$ = 40000K, $\log g$ = 4.0, $M = 30M_{\odot}$). Full line is a model calculated with the help of occupation probabilities, dashed lines denote a model calculated using the standard cutoff procedure. T stands for temperature, and m for the column mass depth.

were assumed to have depth independent Doppler profiles during calculation. Photoionization cross sections are calculated using the occupation probabilities according to the Sect. 2.3. The collisional ionization rates were evaluated using the polynomial fit of Napiwotzki (1993). For the collisional excitation of H I the expressions given in Mihalas (1967) were used. The higher, non-explicit levels were assumed to be in LTE with respect to the next higher ion. The ionization from these levels is taken into account by means of the so-called modified free-free cross-section (Auer & Mihalas 1969a). The collisional transitions between explicit and non-explicit levels are taken into account by means of a modified collisional ionization rate (see Hubeny 1988). The LTE population numbers of both explicit and non-explicit levels were calculated using the occupation probability formalism, as described in the Sect. 2.1.

4.1. Hot main sequence stars

For a sample calculation of model atmospheres of main sequence stars we have chosen $T_{\rm eff}$ = 40000K, $\log g$ = 4.0, $M = 30M_{\odot}$ as an typical O star and $T_{\rm eff}$ = 30000K, $\log g$ = 4.0, $M = 15M_{\odot}$ as a hot B star. The cooler B star of $T_{\rm eff}$ = 20000K, $\log g$ = 4.0 was analysed by HHL. Temperature structures of our resulting spherically symmetric model atmospheres are plotted in Fig. 1 both for the case of occupation probabilities and standard cutoff procedure. For the case of a hotter O star we found the difference only about 0.2%, while for a hot B star the difference is about 0.8% in the outer layers. The hot B star has differing temperatures also at depth about $m \sim 10^{-2}$. Nevertheless, the changes in temperature structure do not affect emergent radiation in lines very much, the differences are hardly visible on a plot. Therefore we do not show them here.

4.2. O subdwarfs

The parameters for a testing of a typical sdO star were taken from Lanz et al. (1997). $T_{\rm eff}$ = 55000K, $\log g$ = 5.5, $M = 0.5M_{\odot}$ correspond to a star BD +75° 325. However, contrary to the real situation, helium was neglected in out test calculations. Similarly to the case of hot main sequence stars, the differences in temperature (see Fig. 2) are present only in the outer layers. However they are slightly higher than in the case of hot main sequence stars, namely about 0.7%. We plotted the Balmer line profiles for both cases in Fig. 3. The differences are hardly visible on a plot.

4.3. White dwarfs

For testing the effect of the occupation probabilities for the case of hot white dwarfs we used following stellar parameters: $T_{\rm eff}$ = 100000K, $\log g$ = 7.5, $M = 0.6M_{\odot}$. Temperature structures of the resulting spherically symmetric model atmospheres are plotted in Fig. 2. The difference caused by improved treatment of the level dissolution is almost negligible, only in the outermost layers we see a difference about 0.3%.

The case of a cooler white dwarf was tested for $T_{\rm eff}$ = 40000K, $\log g$ = 8.0, $M = 0.6M_{\odot}$. We found larger differences in the temperature structure (see Fig. 2) than in the very hot case of $T_{\rm eff}$ = 100000K. These difference in T are about 1.2% in the outer layers.

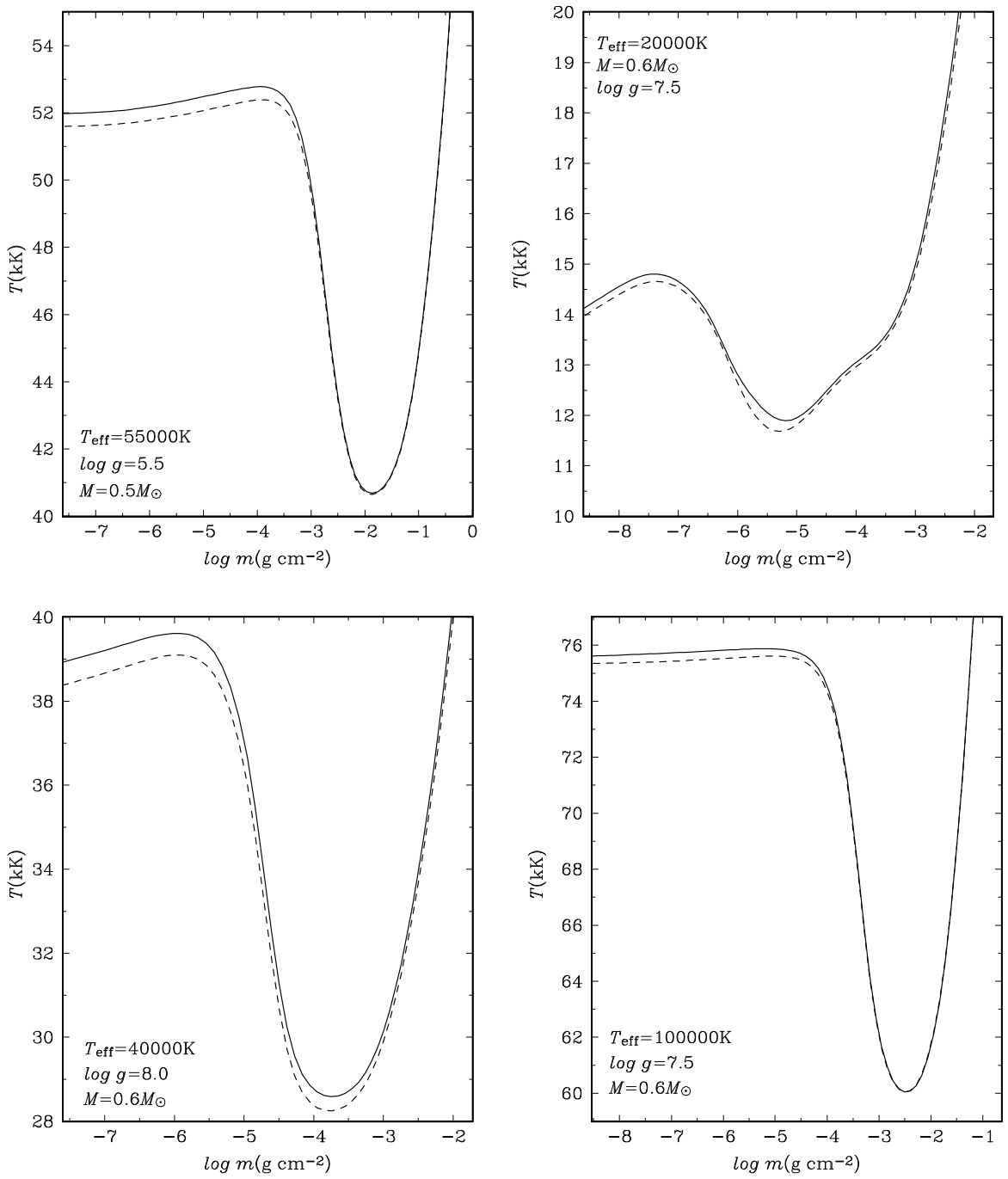

Fig. 2. The same as Fig. 1 for an O subdwarf and for three white dwarfs. The stellar parameters are displayed in the figure.

We also tested the effect of occupation probabilities on the model atmosphere of a cool white dwarf with $T_{\rm eff}$ = 20000K, $\log g$ = 7.5, $M = 0.6 M_\odot$. We found quite interesting behaviour of temperature structures. Both models practically coincide up to the depth where the Lyman continuum is formed ($m \sim 10^{-5}$). There the difference between the occupation probability formalism and the standard cutoff procedure comes into effect. Slightly different absorption cross section in the region of maximum continuum flux causes the quite significant differences displayed in the Fig. 2. The difference of outer temperatures for this particular model is about 1.3%. However, deeper in the atmosphere at $m \sim 10^{-5}$, where the Lyman continuum is formed, the difference has similar value, i.e. it is quite large.

All of these results could be expected. For very hot atmospheres, only a very little amount of hydrogen is not ionized. Consequently, the change in the number of free electrons caused by the occupation probability formalism is very small. This number is larger for a cooler atmosphere of $T_{\rm eff}$ = 40000K,

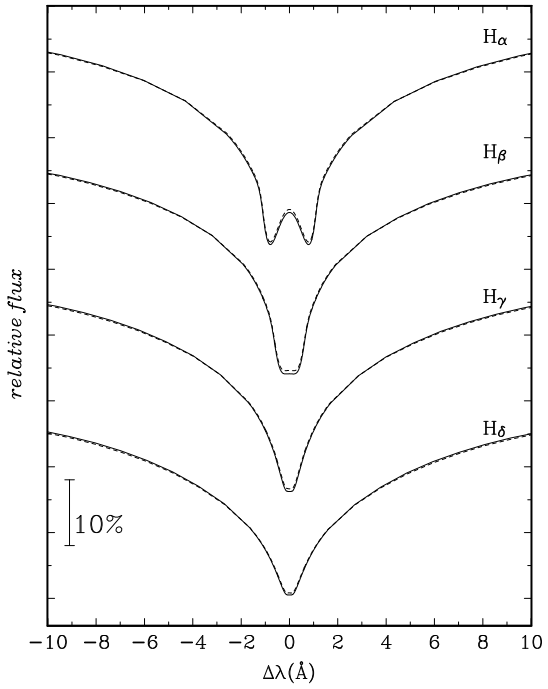

Fig. 3. Balmer line profiles for the O subdwarf model atmospheres with $T_{\rm eff}$ = 55000K, $\log g$ = 5.5, and $M = 0.5 M_{\odot}$. Full lines denote the spectrum emerging from models calculated using the occupation probabilities, dashed lines denote models calculated using the standard cutoff procedure.

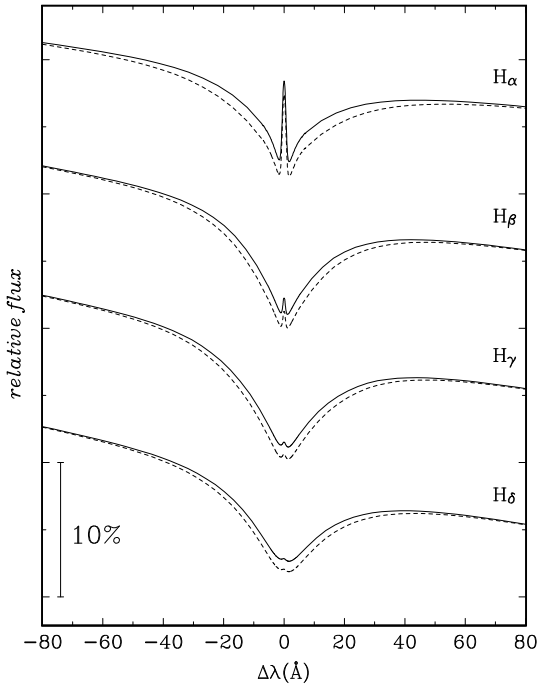

Fig. 4. Balmer line profiles for the white dwarf model atmospheres with $T_{\rm eff}$ = 100000K, $\log g$ = 7.5, and $M = 0.6 M_{\odot}$. Full lines denote the spectrum emerging from models calculated with the help of occupation probabilities, dashed lines denote models calculated using the standard cutoff procedure.

where the amount of neutral hydrogen is larger. Even more neutral hydrogen is present for the coolest model atmosphere we have calculated ($T_{\rm eff}$ = 20000K). The effect of occupation probabilities is quite pronounced for this particular model. One would expect an even larger effect on still cooler atmospheres, but for such atmospheres the effect of convection comes into play and our results would have only academic value.

Since the differences for the white dwarfs are not negligible, we plotted the Balmer line profiles for H_α, H_β, H_γ, and H_δ lines for all of our white dwarf models in Figs.4 – 6. All profiles were normalized to unity continuum flux in the center of a line. The differences for the hottest models ($T_{\rm eff}$ = 100000K) are about 1% in the region about line center. Inclusion of the occupation probability formalism causes the profiles to be shallower. Although this small effect is not drastic, it is much more pronounced than for the case of main-sequence stars. Even more interesting is the behaviour of the line profiles for the model with $T_{\rm eff}$ = 40000K. The region where the profiles differ is broader than for the hottest white dwarf under consideration. Very interesting is the difference in the blue wing of H_δ line. For this particular line (see Fig. 5) another effect of level dissolution comes into a play. The transitions to dissolved levels are photoionizing transitions, and according to the Eqs.(24) and (25) the photoionization cross-section under the ionization edge is larger. Due to the larger continuum opacity the emergent flux is consequently lower. On the other hand, the line profiles of the cool white dwarf of $T_{\rm eff}$ = 20000K (Fig. 6) do not display remarkable differences except the difference in the blue wing of H_δ.

These relatively important differences between occupation probability formalism and standard cutoff procedure have one reason. Relatively large density and pressure in white dwarfs causes the standard cutoff procedure to be less realistic than for main-sequence stars. Hence using the better occupation probability formalism has a pronounced effect for white dwarfs.

In order to see the direct effect of the difference between the occupation probability formalism and cutoff procedure on the ionization and electron density, we plotted the depth dependence of the electron density for both cases in the upper panel of Fig. 7. No difference can be seen on the logarithmic scale. Therefore we plotted the relative differences in the lower panel of Fig. 7. The differences are of the order of percent reaching a maximum of about 3% for $m \sim 10^{-1}$, i.e. at the continuum forming region.

5. Conclusions

In this paper we have described the implementation of the NLTE occupation probability formalism into the equations of statistical equilibrium. We used the method of HHL. However, we included the occupation probabilities into the rates and we refer to these modified quantities as to the "weighted rates" (Eqs.(6) – (10)).

With this improved formulation of the equations of statistical equilibrium, and of the equations for the opacities, we calcu-

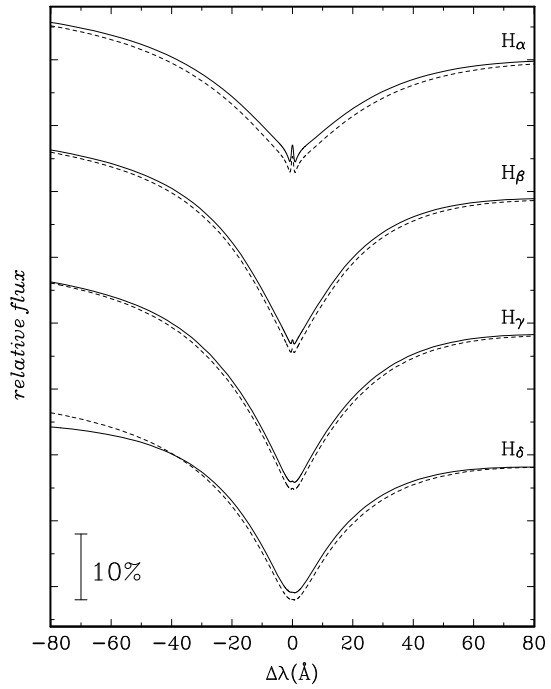

Fig. 5. The same as Fig. 4 for $T_{\rm eff}$ = 40000K, $\log g$ = 8.0, and $M = 0.6 M_\odot$.

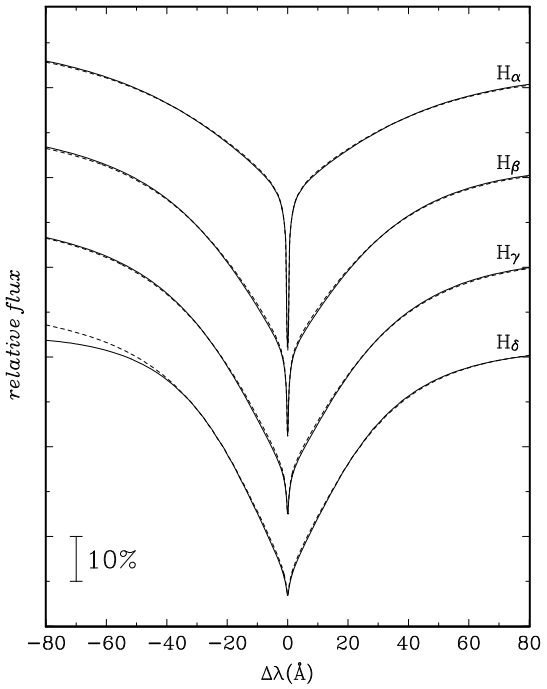

Fig. 6. The same as Fig. 4 for $T_{\rm eff}$ = 20000K, $\log g$ = 7.5, and $M = 0.6 M_\odot$.

lated a small set of model atmospheres to test the effect of proper treatment of a level dissolution when compared to the "classical" treatment with the help of the standard cutoff method. We found (similarly to HHL) that for hot main sequence stars the difference is very small and is hardly visible on a plot of line profiles. A very small difference was found also for a subdwarf O star. On the other hand, the largest effect was found for white dwarfs. We conclude that especially for this class of stars it is necessary to use of the occupation probability formalism in the calculation of ionization balance (both LTE and NLTE), statistical equilibrium, and opacities.

Acknowledgements. The author would like to thank Drs. David Holmgren and Frédéric Paletou for their comments on the manuscript. A part of the calculations presented in this paper was carried out on the Cray YMP-EL computer of the Institute of Physics of the Academy of Sciences of the Czech Republic. This work was supported by an internal grant of Academy of Sciences of the Czech Republic C3003601, by a grant of the Grant Agency of the Czech Republic (GA ČR) 205/96/1198, and by projects K1-003-601/4 and K1-043-601.

Appendix A: details of the linearization

After discretization and linearization of all equations, we obtain a tridiagonal system of the form

$$\mathbf{A}_d \delta\boldsymbol{\psi}_{d-1} + \mathbf{B}_d \delta\boldsymbol{\psi}_d + \mathbf{C}_d \delta\boldsymbol{\psi}_{d+1} = \boldsymbol{L}_d,$$

and $\mathbf{A}_1 = \mathbf{C}_{ND} = 0$ (ND is the number of depth points). This system is solved by standard Gaussian elimination (see Paper I). Since the expressions for the linearized equations of hydrostatic and radiative equilibrium were presented in Papers I and II, we present only the expressions for the equations of statistical equilibrium here.

A.1. Explicit linearization of the equations of statistical equilibrium

Eq.(29) yields the particular coefficients (x stands for n_e or T) of the form

$$\left(\mathbf{A}_x^{SE(j)}\right)_d = \sum_{l=1}^{NL} \left.\frac{\partial \mathscr{A}_{jl,d}}{\partial x}\right|_{d-1} b_{l,d} \tag{A1}$$

$$\left(\mathbf{B}_x^{SE(j)}\right)_d = \sum_{l=1}^{NL} \left.\frac{\partial \mathscr{A}_{jl,d}}{\partial x}\right|_{d} b_{l,d} - \left.\frac{\partial \mathscr{B}_{j,d}}{\partial x}\right|_{d} \tag{A2}$$

$$\left(\mathbf{C}_x^{SE(j)}\right)_d = \sum_{l=1}^{NL} \left.\frac{\partial \mathscr{A}_{jl,d}}{\partial x}\right|_{d+1} b_{l,d} \tag{A3}$$

$$\left(\mathbf{A}_{b_k}^{SE(j)}\right)_d = \sum_{l=1}^{NL} \left.\frac{\partial \mathscr{A}_{jl,d}}{\partial b_k}\right|_{d-1} b_{l,d} \tag{A4}$$

$$\left(\mathbf{B}_{b_k}^{SE(j)}\right)_d = \sum_{l=1}^{NL} \left.\frac{\partial \mathscr{A}_{jl,d}}{\partial b_k}\right|_{d} b_{l,d} + A_{jk,d} - \left.\frac{\partial \mathscr{B}_{j,d}}{\partial b_k}\right|_{d} \tag{A5}$$

$$\left(\mathbf{C}_{b_k}^{SE(j)}\right)_d = \sum_{l=1}^{NL} \left.\frac{\partial \mathscr{A}_{jl,d}}{\partial b_k}\right|_{d+1} b_{l,d} \tag{A6}$$

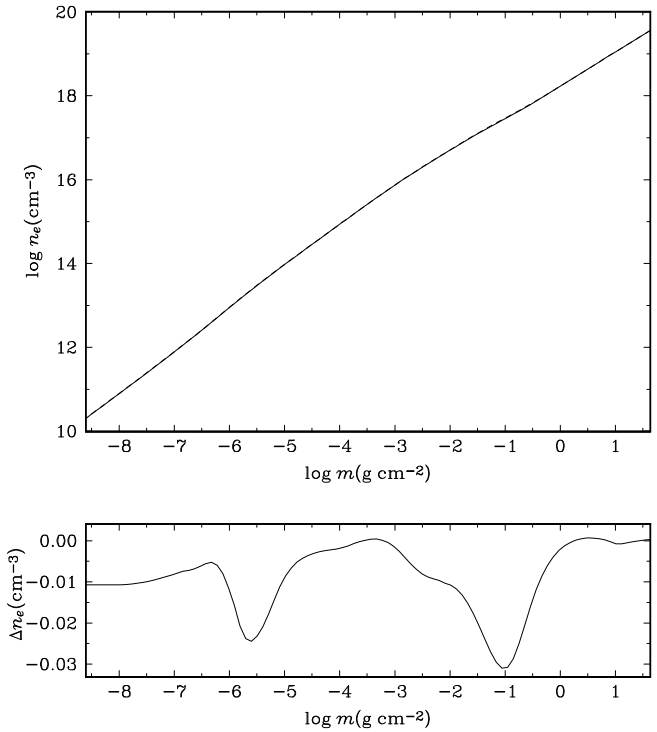

Fig. 7. The effect of the occupation probabilities on the electron density for the case of a white dwarf model atmosphere with $T_{\rm eff}$ = 20000K, $\log g$ = 7.5, and $M = 0.6 M_\odot$. The electron structure is plotted in the upper panel both for the case of occupation probability formalism and standard cutoff procedure. Plotted on a logarithmic scale both curves coincide. On the lower panel we have plotted the relative difference between both cases.

$$\left(\mathbf{L}^{SE(j)}\right)_d = \mathscr{B}_{j,d} - \sum_{l=1}^{NL} \mathscr{A}_{jl,d} b_{l,d} \tag{A7}$$

The nonlocal terms in off-diagonal elements arise from the tridiagonal operator. For diagonal operators actually vanish.

A.2. Implicit linearization of the equations of statistical equilibrium

For the implicit linearization we do not write any linearization coefficients for the equations of statistical equilibrium, since we do not linearize them explicitly. They are linearized indirectly with a help of the derivatives of *b*-factors – see Eq.(31).

A.3. The derivatives of the rate matrix

Let us express the derivatives of rate matrix coefficients explicitly. The derivatives of the rate matrix coefficients are simply (y stands for n_e, T, b_i)

$$\frac{\partial \mathscr{A}_{ii}}{\partial y} = \sum_{l=1}^{NL} \frac{\partial(\tilde{R}_{il} + \tilde{C}_{il})}{\partial y} \tag{A8}$$

for diagonal elements, and

$$\frac{\partial \mathscr{A}_{il(i\neq l)}}{\partial y} = -\frac{\partial(\tilde{R}_{li} + \tilde{C}_{li})}{\partial y} \tag{A9}$$

for non-diagonal elements. The derivatives of particular rates are (x stands for n_e, T)

$$\frac{\partial \tilde{R}_{il}}{\partial x} = \frac{4\pi}{h\nu_{il}} n_i^* w_l \int_0^\infty \sigma_{il}(\nu) \Lambda_\nu^* \frac{\partial S_\nu}{\partial x} \mathrm{d}\nu + \frac{1}{n_i^*} \frac{\partial n_i^*}{\partial x} \tilde{R}_{il} \tag{A10}$$

for upward (both bound-bound and bound-free) radiative rates,

$$\frac{\partial \tilde{R}_{li}}{\partial x} = \frac{4\pi}{h\nu_{il}} n_l^* w_i \frac{g_i}{g_l} \int_0^\infty \sigma_{il}(\nu) \Lambda_\nu^* \frac{\partial S_\nu}{\partial x} \mathrm{d}\nu + \frac{1}{n_l^*} \frac{\partial n_l^*}{\partial x} \tilde{R}_{li} \tag{A11}$$

for downward bound-bound rates, and

$$\frac{\partial \tilde{R}_{li}}{\partial x} = 4\pi n_i^* w_i \int_0^\infty \frac{\sigma_{il}(\nu)}{h\nu} \Lambda_\nu^* \frac{\partial S_\nu}{\partial x} e^{-h\nu/kT} \mathrm{d}\nu + \frac{1}{n_i^*} \frac{\partial n_i^*}{\partial x} \tilde{R}_{li} + \delta_{Tx} 4\pi n_i^* w_i \int_0^\infty \frac{\sigma_{il}(\nu)}{kT^2} \times \left(\frac{2h\nu^3}{c^2} + \Lambda_\nu^* S_\nu + \Delta J_\nu \right) e^{-h\nu/kT} \mathrm{d}\nu \tag{A12}$$

for free-bound rates. Here $\delta_{Tx} = 1$ for $x = T$ and 0 otherwise. For derivatives versus *b*-factors hold

$$\frac{\partial \tilde{R}_{il}}{\partial b_m} = \frac{4\pi}{h\nu_{il}} n_i^* w_l \int_0^\infty \sigma_{il}(\nu) \Lambda_\nu^* \frac{\partial S_\nu}{\partial b_m} \mathrm{d}\nu \tag{A13}$$

for upward (both bound-bound and bound-free) radiative rates,

$$\frac{\partial \tilde{R}_{li}}{\partial b_m} = \frac{4\pi}{h\nu_{il}} n_l^* w_i \frac{g_i}{g_l} \int_0^\infty \sigma_{il}(\nu) \Lambda_\nu^* \frac{\partial S_\nu}{\partial b_m} \mathrm{d}\nu \tag{A14}$$

for downward bound-bound rates, and

$$\frac{\partial \tilde{R}_{li}}{\partial b_m} = 4\pi n_i^* w_i \int_0^\infty \frac{\sigma_{il}(\nu)}{h\nu} \Lambda_\nu^* \frac{\partial S_\nu}{\partial b_m} e^{-h\nu/kT} \mathrm{d}\nu \tag{A15}$$

for free-bound rates. The derivatives of collisional rates read

$$\frac{\partial \tilde{C}_{il}}{\partial n_e} = \frac{\partial \tilde{C}_{li}}{\partial n_e} = \frac{1}{n_i^*} \frac{\partial n_i^*}{\partial n_e} \tilde{C}_{il} + n_i^* w_l q_{il}(T) \tag{A16}$$

$$\frac{\partial \tilde{C}_{il}}{\partial T} = \frac{\partial \tilde{C}_{li}}{\partial T} = \frac{1}{n_i^*} \frac{\partial n_i^*}{\partial T} \tilde{C}_{il} + n_i^* w_l n_e \frac{\partial q_{il}(T)}{\partial T} \tag{A17}$$

$$\frac{\partial \tilde{C}_{il}}{\partial b_m} = \frac{\partial \tilde{C}_{li}}{\partial b_m} = 0 \tag{A18}$$

both for upward and downward rates. The derivatives for the closing equations of charge conservation, particle conservation, and abundance, follow directly from Eqs. (18) – (20).

References

Auer L.H., 1976, JQSRT 16, 931
Auer L.H., Mihalas D., 1969a, ApJ 156, 157
Auer L.H., Mihalas D., 1969b, ApJ 158, 641
Däppen W., Anderson L.S., Mihalas D., 1987, ApJ 319, 195
Däppen W., Mihalas D., Hummer D.G., Mihalas B.W., 1988, ApJ 332, 261
Feautrier P., 1964, C. R. Acad. Sci. Paris, 258, 3189
Gallagher J.W., Pradhan A.K., 1985, JILA Data Center Report No.30, University of Colorado
Hubeny I., 1988, Comput. Phys. Commun. 52, 103
Hubeny I., Hummer D.G., Lanz T., 1994, A&A 282, 151 (HHL)
Hummer D.G., Mihalas D., 1988, ApJ 331, 794
Kubát J., 1994, A&A 287, 179 (Paper I)
Kubát J., 1995, A&A 299, 803
Kubát J., 1996, A&A 305, 255 (Paper II)
Kubát J., 1997, A&A, in press
Kudritzki R.P., Hummer D.G., 1990, ARA&A 28, 303
Lanz T., Hubeny I., Heap S., 1997, ApJ, submitted
Menzel D.H., 1937, ApJ 85, 330
Mihalas D., 1967, ApJ 149, 169
Mihalas D., 1978, Stellar Atmospheres, 2nd ed., W.H.Freeman & Comp., San Francisco
Mihalas D., 1985, J. Comput. Phys. 57, 1
Mihalas D., Auer L.H., 1970, ApJ 160, 1161
Mihalas D., Däppen W., Hummer D.G., 1988, ApJ 331, 815
Mihalas D., Hummer D.G., Mihalas B.W., Däppen W., 1990, ApJ 350, 300
Napiwotzki R., 1993, Ph.D. thesis, Universität Kiel
Olson G.L., Kunasz P.B., 1987, JQSRT 38, 325
Puls J., 1991, A&A 248, 581
Rybicki G.B., Hummer D.G., 1991, A&A 245, 171
Traving G., Baschek B., Holweger H., 1966, Abh. Hamburger Sternwarte VIII, No.1
Werner K., 1996, A&A 309, 861
Wiese W.L., Smith M.W., Glennon B.M., 1966, Atomic Transition Probabilities, Vol.I., Hydrogen Through Neon, NSRDS-NBS 4, Washington D.C.

This article was processed by the author using Springer-Verlag LaTeX A&A style file *L-AA* version 3.